Published in final edited form as:
Int J Radiat Oncol Biol Phys. 2011 March 1; 79(3): 948–955. doi:10.1016/j.ijrobp.2010.05.062.

Post-Lumpectomy Focal Brachytherapy for Simultaneous Treatment of Surgical Cavity and Draining Lymph Nodes

Brian A. Hrycushko, M.S.[*], **Shihong Li, Ph.D.**[*], **Chengyu Shi, Ph.D.**[†], **Beth Goins, Ph.D.**[*], **Yaxi Liu, Ph.D.**[†], **William T. Phillips, M.D.**[*], **Pamela M. Otto, M.D.**[*], and **Ande Bao, Ph.D.**[*,‡]

[*]Department of Radiology, University of Texas Health Science Center at San Antonio, San Antonio, Texas

[†]Department of Radiation Oncology, University of Texas Health Science Center at San Antonio, San Antonio, Texas

[‡]Department of Otolaryngology – Head and Neck Surgery, University of Texas Health Science Center at San Antonio, San Antonio, Texas

Abstract

Purpose—The primary objective was to investigate a novel focal brachytherapy technique using lipid nanoparticle (liposome)-carried β-emitting radionuclides (rhenium-186 [^{186}Re]/rhenium-188 [^{188}Re]) to simultaneously treat the post-lumpectomy surgical cavity and draining lymph nodes.

Methods and Materials—Cumulative activity distributions in lumpectomy cavity and lymph nodes were extrapolated from small animal imaging and human lymphoscintigraphy data. Absorbed dose calculations were performed for lumpectomy cavities with spherical and ellipsoidal shapes and lymph nodes within human subjects using the dose point kernel convolution method.

Results—Dose calculations showed that therapeutic dose levels within the lumpectomy cavity wall can cover 2 and 5 mm depths for ^{186}Re- and ^{188}Re-liposomes, respectively. The absorbed doses at 1 cm sharply decreased to only 1.3 – 3.7% of the doses at 2 mm for ^{186}Re-liposomes and 5 mm for ^{188}Re-liposomes. Concurrently, the draining sentinel lymph nodes would receive a high focal therapeutic absorbed dose, while the average dose to 1 cm of surrounding tissue received < 1% of that within the nodes.

Conclusions—Focal brachytherapy using ^{186}Re/^{188}Re-liposomes was theoretically shown capable of simultaneously treating the lumpectomy cavity wall and draining sentinel lymph nodes with high absorbed doses while significantly lowering dose to surrounding healthy tissue. In turn, this allows for dose escalation to regions of higher probability of containing residual tumor cells following lumpectomy while reducing normal tissue complications.

Keywords

Breast cancer; Lymph node; Focal brachytherapy; Liposome; Radionuclide

Reprint requests to: Ande Bao, Ph.D., Department of Radiology, University of Texas Health Science Center at San Antonio, 7703 Floyd Curl Drive, MSC 7800, San Antonio, TX 78229-3900; Tel: (210) 567-5657; Fax: (210) 567-5549; bao@uthscsa.edu.

Conflict of interest: none.

Introduction

Most women (75%) diagnosed with breast cancer are of early stage due to advances in screening and have the possibility of being treated with lumpectomy or other forms of breast conserving therapy (1). Breast conserving therapy results in a superior cosmetic outcome, thus increasing overall quality of life. The rationale of breast conserving therapy has been investigated through 20-year follow-up studies which have shown similar survival rates after either lumpectomy followed by radiotherapy or mastectomy (2,3). The majority of recurrences after lumpectomy appear at or in close proximity to the tumor bed and surgical scar (1,4,5) indicating a high probability of residual tumor clonogens within the vicinity. This is the basis for partial breast irradiation or boost fields which localize radiation beams and escalate absorbed dose to the tumor bed. The new technique evaluated in this work is based on the hypothesis that further dose escalation to the tumor bed through focal irradiation while minimizing dose to the rest of the breast will reduce local recurrences, increase overall survival, and reduce normal tissue complications (6).

In addition, lymphatic vessels within the breast provide pathways for tumor cell invasion and migration to regional lymph nodes, which can result in tumor metastases. Evidence has indicated that micrometastases or isolated tumor cells within the lymph nodes is associated with a reduced rate in 5-year disease free survival if no additional treatment is given (7). Axillary radiotherapy is an attractive alternative to axillary dissection, attaining similar survival rates with an improved quality of life (8). However, complications after axillary irradiation are determined by the important structures irradiated (brachial plexus, axillary vessels, and lymphatics). Minimizing the radiation delivered to adjacent healthy tissue is expected to reduce morbidity. An aim of the treatment method described in this work is the simultaneous focal irradiation of the sentinel lymph nodes within the lymphatic chain accompanying the irradiation of the lumpectomy cavity. This is expected to reduce the risk of tumor cell metastatic spread after lumpectomy, while tissue surrounding the lymph nodes and uninvolved lymphatics will experience a minimal absorbed dose compared with current axillary irradiation techniques.

Herein, a novel approach to simultaneously treat the post-lumpectomy tumor bed and draining sentinel lymph nodes using ^{186}Re/^{188}Re-liposomes is reported. Liposomes are nano-scale biodegradable lipid vesicles proven in their effectiveness and safety as drug delivery vehicles for treatment of human disease (9). They are used as carriers of the radionuclides due to increased retention within the injection region and lymph nodes compared with non-liposomal radionuclide compounds (10-12). This allows for more absorbed dose to be delivered to desired targets and less dose to be given to normal tissue. Fig. 1 illustrates the overall treatment strategy. Specifically: 1) A therapeutic dose of liposomal radionuclides is injected into the lumpectomy cavity; 2) Sustained retention of liposomes within the cavity delivers a therapeutic absorbed dose to the cavity wall and surrounding tissue; 3) Liposomes slowly drain from the cavity through lymphatic and blood vessels; 4) The particulate liposomes are filtered by lymph nodes (13, Fig. 2) in a similar distribution pattern as microscopic tumor; and 5) Retained liposomes focally treat the entire lymph node to a therapeutic dose level. This design is evaluated using observations from small animal imaging studies and human lymphoscintigraphy data as input for absorbed dose calculations using a Monte Carlo simulation code and numerical integration methods utilizing dose point kernels (DPKs).

Methods and Materials

Dose Point Kernels

The radionuclide DPK convolution method, which is based on convolving a radionuclide DPK with a cumulative activity distribution, is used to calculate dose distributions. Convolution mathematics is a quick and easy method of evaluating absorbed dose calculations for radionuclide therapy (14,15). The EGSnrc Monte Carlo simulation (16)user code EDKnrc (17) was used to calculate DPKs which included absorbed dose from photon and beta emissions (18,19) of ^{186}Re and ^{188}Re radionuclides. DPKs of selected radionuclides, and mono-energy photons and electrons were also calculated within a water medium for validation of accuracy with published DPKs (20-24).

The DPK convolution technique inherently assumes a spatially invariant dose kernel within a uniform homogeneous medium and often is used as a quick approximation within heterogeneous media. To use the convolution technique, the feasibility of using a homogeneous assumption for breast dosimetry was determined. DPKs for ^{186}Re and ^{188}Re were generated and compared using the PEGS4 (16) data sets for different materials which may represent breast tissue compositions and heterogeneities: soft tissue, adipose tissue, glandular tissue, breast tissue, water, and a BR12 breast tissue phantom.

Lymph Node Dose Calculations

Dose calculation utilizing the DPK convolution technique has previously been described (14) and only a brief explanation follows. Three-dimensional 500×500×500 matrices with voxel sizes of 0.2×0.2×0.2 mm^3 were formulated in Matlab (ver. 7.4.0.287 [R2007a]). The DPK matrix (K; mGy/MBq/hr) was formulated using the DPK data for the radionuclides in water, while the cumulative activity matrix ($\tilde{A}$; MBq•hr) was the cumulative activity distribution within a lymph node. The lymph node was modeled as disk shaped having an 8 mm diameter and 4 mm height to represent a normal lymph node in the human body. The clinical basis for choosing this was that enlarged lymph nodes would typically be dissected and the lymph node treatment should target involved sentinel lymph nodes without apparent changes in nodal size to eradicate isolated tumor cells or micrometastases. An exponentially decreasing cumulative activity distribution from the subcapsular sinus region within the lymph nodes was assumed. This model was derived from our observations from fluorescent imaging of the distribution of the liposomes labeled with rhodamine B within rat lymph nodes (Fig. 2). The majority of liposomes were retained in the outer rim, and this distribution has also been previously documented (13). This declining liposomal density distribution may be attributed to the filtering mechanism of the lymph nodes as lymphatic fluid permeates the sinuses.

The convolution of the DPK matrix with the cumulative activity matrix was calculated using Fourier transform (FT), multiplication (•), followed by inverse Fourier transform (iFT) (14,15):

$$D(i,j,k) = iFT\left\{FT\left[K(i,j,k)\right] \bullet FT\left[\tilde{A}(i,j,k)\right]\right\}$$

where i, j, and k are voxel indices. The amount of cumulative activity distributed within the lymph node model was chosen to deliver an average absorbed dose of 150 Gy to the lymph node. This absorbed dose level was chosen as an acceptable focal dose level to treat the entire lymph node; being large enough to treat the entire lymph node to a large dose, yet low enough to spare surrounding tissue. From this desired absorbed dose and the assumptions

described in the following section, the amount of activity administered to the lumpectomy cavity to deliver this absorbed dose was determined.

Lumpectomy Cavity Dose Calculations

The DPK convolution method was also applied to calculate absorbed dose within the lumpectomy cavity and the cavity wall. The effect of lumpectomy cavity size on absorbed dose to the cavity wall was evaluated by modeling different sized spherical geometry cavities of 1.0 and 1.5 cm in diameter containing uniformly distributed cumulative activity. Although the volume of the excised tumor and tumor free margins may be much larger, lumpectomy cavities should be compressed after tumor excision due to lack of tissue support within the cavity, markedly decreasing cavity volume. This has been seen in cavity volume quantification studies, and in some cases an almost planar geometry is seen with thicknesses on the order of millimeters (25). The amount of cumulative activity uniformly distributed within the cavity was determined from the calculated amount of cumulative activity needed to give the average dose of 150 Gy to the post-lumpectomy sentinel lymph node and assuming an average of 0.5% of the injected activity was retained by the lymph node. This conservative percentage is extrapolated from findings in human radiocolloid and liposomal lymphoscintigraphy studies (12,26). The amount of injected activity within the lumpectomy cavity was calculated utilizing the intracavitary retention data from small animal imaging studies which determined the percentage of injected radioactivity within the rat lumpectomy cavity over time. The biological half-life of the liposomal radioactivity within the lumpectomy cavity was determined to be approximately 50 hours, which was similar to that seen for intraoperative delivery of ^{186}Re-liposomes for head and neck cancer (27).

An ellipsoidal cavity with the same volume as the 1.5 cm diameter sphere was created having a major axis three times the size of the minor axis to represent a collapsed cavity following lumpectomy. The cavity was uniformly given the same amount of cumulative activity as that of the 1.5 cm diameter sphere, and the absorbed dose distribution was also calculated. The distribution of absorbed dose within the surrounding tissue was analyzed to determine how collapsed lumpectomy cavities would affect dose uniformity and treatment delivery protocol.

Targeting Liposomes

An important characteristic of liposomes is that they may be modified with different surface charges or specific targeting molecules on the liposomal surface. For example, antibodies may be used to target liposomes to specific cells within the body (28), or liposomal surface charge may be modified to alter uptake and accumulation characteristics within tissue. Evidence has shown that cationic liposomes possibly collect along the surface of the lumpectomy cavity wall (27,29). This passive targeting of the wall may be due to the negative surface charge of typical cell membranes (30). Whether by antibody or charge modification techniques, a 1.5 cm diameter sphere was modeled to have all the cumulative activity inside the cavity within 1 mm of the wall surface representing surface modified ^{186}Re/^{188}Re-liposomes. The DPK convolution method was used to calculate the cavity wall absorbed dose distribution for comparison with the same size sphere having the same amount of cumulative activity uniformly distributed.

Results

Dose Point Kernels

The DPKs within various media representing breast tissue or similar compositions are shown in Fig. 3. A semi-log plot is used to display entire DPKs, illustrating the sharp decrease in dose delivered primarily through beta-radiation within a few mm. This beta

range is followed by low absorbed dose contributed mainly by photon-radiation (x- and gamma-rays) with an approximate $1/r^2$ decrease with distance. The beta-radiation ranges are around 4.5 and 9.5 mm for ^{186}Re and ^{188}Re, respectively, with the remaining almost-negligible bremmstrahlung radiation doses beyond these distances. The absorbed dose-distance pattern results in effective therapeutic absorbed doses given within mm ranges while doses outside this range rapidly decrease to minimal levels. Thus a focal treatment is achieved resulting in greatly decreased surrounding normal tissue toxicity.

DPKs for all media were similar within 2 and 5 mm range for ^{186}Re and ^{188}Re respectively; however, the BR12 breast tissue phantom and adipose tissue had higher absorbed doses beyond these distances within the range of beta-radiation. These differences are quantified in Fig. 4, which compares the percent difference of each DPK with the DPK in water. Water was used for comparison as it is often the preferred phantom medium in radiotherapy protocols. The largest difference (approaching 80%) compared to that of water is seen with adipose tissue and the BR12 breast tissue phantom; however, the distance at which the largest differences occur would receive minimal dose levels and should not significantly influence the absorbed dose calculations (see calculated absorbed dose data in sections below). The difference between the DPKs within the PEGS4 breast tissue composition and that for water is very low (approaching 3.5% within the therapeutic ranges (see below)), showing that a homogeneous water phantom is more appropriate than the adipose tissue and the BR12 breast tissue phantom to represent breast tissue for radionuclide therapy dosimetry.

Lymph Node Absorbed Dose

Fig. 5 and Table 1 depict the absorbed dose distribution within a lymph node as well as in the surrounding normal tissue. The dose profile along the central slice within the lymph node (Fig. 5A) shows that there were minimum doses in the outer capsule (± 4 mm) and medulla regions for the described cumulative activity distribution within the lymph node. However, although the majority of the liposomes accumulate within the outer rim, the beta emissions from both ^{186}Re and ^{188}Re are able to treat the entire lymph node to therapeutic dose levels. This is achieved while providing a steep decline in absorbed dose within a few mm of surrounding tissue. Fig. 5B shows dose volume histograms (DVHs) for the lymph node and surrounding 1 cm thickness of healthy tissue for both radionuclides. The DVHs show that ^{188}Re-liposomes can deliver a more uniform dose to the lymph node due to the more energetic beta-radiation from ^{188}Re. The DVHs for the surrounding 1 cm of tissue show that absorbed dose is minimal compared to levels within the lymph node, demonstrating the tissue sparing capability of liposome-carried radionuclides. This is further exemplified in Table 1, which gives absorbed doses seen within the lymph node and at incremental distances within the surrounding tissue. The less energetic beta-radiation from ^{186}Re delivers a higher maximum dose in order to achieve 150 Gy of average lymph node dose. The tissue sparing effect of both radionuclides is evident with the average absorbed dose within 1 cm of surrounding tissue being over three orders of magnitude less than the average dose within the lymph node.

Lumpectomy Cavity Absorbed Dose

Table 2 lists point doses at specified depths from the wall surface surrounding the spherical lumpectomy cavity. The therapeutic ranges of 2 and 5 mm for ^{186}Re and ^{188}Re, respectively, are also shown from the dose calculations. Table 2 illustrates that dose levels at further distances are inadequate to kill clusters of residual tumor clonogens. The amount of injected activity was determined to be 29.1 and 42.9 mCi for ^{186}Re- and ^{188}Re-liposomes, respectively. The smaller cavity size could receive a much larger dose to the tumor bed,

showing the importance of knowing cavity volume for treatment planning purposes, as well as ensuring to remove air in the surgical cavity during the delivery of therapeutic agents.

Absorbed dose distributions seen at distances from the ellipsoidal (collapsed) shaped lumpectomy cavity are given in Table 3. The absorbed dose to tissue surrounding the short axis of the lumpectomy cavity is much greater than that received by tissue surrounding the long axis. This demonstrates that collapsed cavities with uniformly distributed cumulative activity will have non-uniform absorbed dose distributions within the surrounding tissue. This will likely affect the injection protocol if a more uniform dose distribution or specific dose level is desired.

Absorbed Dose with Targeting Liposomes

Dose profiles across the center slices of the 1.5 cm spherical lumpectomy cavities containing liposomes with uniform cumulative activity distributions or modified liposomes with cumulative activity distributions targeting the cavity wall are shown in Fig. 6. A uniform distribution of liposomes gives a uniform dose distribution inside the cavity whereas the surface modified liposomes which attach along the cavity wall give a non-uniform dose distribution within the cavity. However, the targeting liposomes are able to treat the surrounding tissue to much higher dose levels, as indicated in Table 4. The average absorbed dose to the surrounding tissue, within the therapeutic range of the radionuclides, increased by approximately 150% and 80% for ^{186}Re- and ^{188}Re-surface modified liposomes, respectively.

Discussion

This absorbed dose calculation study serves as the groundwork for a novel therapy technique focally treating regions having high probability of containing residual cancer cells following early stage breast cancer lumpectomy surgery. The intracavitary administration of ^{186}Re/^{188}Re-liposomes to simultaneously treat the lumpectomy cavity as well as the draining sentinel lymph nodes was shown to be theoretically feasible. The drainage and accumulation of ^{186}Re/^{188}Re-liposomes along involved lymphatics (12) hypothetically allows for the eradication of tumor cells which may migrate and reside in lymphatics leading to lymph node and distant metastases (7,31,32), while the nearby uninvolved lymphatics are spared. This therapy technique may benefit patients by providing a decreased probability of recurrence and fewer treatment complications compared with currently available adjuvant modalities.

The DPK convolution method was shown to be a valid dose calculation approximation within the breast. Although used for homogeneous media, this technique's use was shown rational for breast tissue despite some tissue heterogeneity and possible variations in breast composition among patients. Lumpectomy cavities in close proximity to lung pleura, ribs, or skin will have larger dose inhomogeneities making the DPK convolution technique less accurate. However, the tissue sparing by beta emissions allows treatment in close proximity to these tissues as opposed to current breast conserving brachytherapy methods (33,34) due to much less healthy tissue volume receiving elevated dose levels.

Both ^{186}Re and ^{188}Re radionuclides were shown to be able to deliver large therapeutic doses to the surrounding tissue of the lumpectomy cavity while treating the entire draining sentinel lymph nodes to a therapeutic focal dose. This has important ramifications as it has been described that over 90% of recurrences are seen at or near the tumor bed and surgical scar (35), while lymph nodes are possible routes of metastatic spread. Micrometastases or isolated tumor cells may have the possibility of leading to recurrence and distant metastases if not treated (7).

The use of liposomes as vehicles to carry radionuclides allows for further formulation modifications to alter uptake and accumulation characteristics. The ability to alter the surface of the nano-sized liposomes allows for specific tumor cell / tissue targeting, prolonged retention within injected regions, and accumulation within regional lymphatics. This will allow for even greater therapeutic effect while further reducing normal tissue toxicity.

Treatment planning will be an important aspect of this procedure as in any modality. It was seen that absorbed dose to the targeted regions depends on the injected activity, cavity size and shape, individual kinetics, and activity retention distributions. An important characteristic of both radionuclides is that their main photon emissions (10% 137 KeV gamma-emission for ^{186}Re and 15% 155 KeV gamma-emission for ^{188}Re) are of similar energy to that emitted by ^{99m}Tc. Furthermore, the chemistry used for the preparation of ^{186}Re/^{188}Re-liposomes may also be used to prepare ^{99m}Tc-liposomes (10). These unique features allow for pre-treatment tracer evaluations using either ^{99m}Tc/^{186}Re/^{188}Re-liposomes for individual kinetics to aid in the treatment planning process and post-treatment imaging evaluation of ^{186}Re/^{188}Re-liposomes for individual absorbed dose calculations.

The short therapeutic range of these radionuclides has been debated for many partial breast irradiation techniques. The “correct” distance from the lumpectomy cavity that one must treat for residual disease is controversial and perceived as a “paradox of local recurrence” (35). Remaining tumor foci after lumpectomy may be found at distances much further than that typically treated with partial breast irradiation techniques (36,37); however, rate of failure elsewhere in the breast seems to be unaffected by whole breast radiotherapy. It seems these remaining microscopic lesions do not manifest clinically under conditions of an unstimulated environment. Moreover, most manifested recurrences are in close proximity to the lumpectomy cavity.Interestingly enough, it has been seen that wound fluid harvested from breast cancer patients stimulates cancer growth *in vitro*, and this stimulatory effect was suppressed if intraoperative irradiation had been used immediately after lumpectomy (38). This suggests that a possible mechanism for the close proximity of recurrences may be suppressed through immediate irradiation of the post-surgical cavity wall. An alternative explanation to the close proximity of recurrences is that trauma to the tumor during surgery may allow cancer cell detachment and may explain the high incidence of positive findings seen in lavage cytology and cavity re-excisions (39,40).

Conclusions

Absorbed dose calculations based on observations from small animal studies and human lymphoscintigraphy data demonstrate that ^{186}Re/^{188}Re-liposomes provide an alternative means of early stage breast cancer treatment post-lumpectomy. The use of radionuclides encapsulated within liposomes offers improvements to proven partial breast irradiation techniques by simultaneously delivering a large absorbed dose to locations having higher probability of containing residual tumor cells following lumpectomy surgery.

This novel technique was shown theoretically feasible to focally treat the lumpectomy cavity wall while minimizing dose to the rest of the healthy breast. At the same time, ^{186}Re/^{188}Re-liposomes which clear to the draining lymph nodes are able to deliver a therapeutic dose to the lymph nodes within the lymphatic chain which are most likely to develop micrometastases. The results of this groundwork study have shown the feasibility for future clinical investigations utilizing this focal breast cancer brachytherapy technique.

Acknowledgments

Supported by Susan G. Komen for the Cure Grant BCTR0707169 and the National Cancer Institute of National Institute of Health (NIH) Grant R01 CA131039. Brian A. Hrycushko was supported by the National Institute of Biomedical Imaging and Bioengineering (NIBIB) of NIH training grant, T-32 EB000817.

References

1. Moore-Higgs GJ. Radiation options for early stage breast cancer. Semin Oncol Nurs 2006;22:233–241. [PubMed: 17095399]
2. Fisher B, Anderson S, Bryant J, et al. Twenty-year follow-up of a randomized trial comparing total mastectomy, lumpectomy, and lumpectomy plus irradiation for the treatment of invasive breast cancer. N Engl J Med 2002;347:1233–1241. [PubMed: 12393820]
3. Veronesi U, Cascinelli N, Mariani L, et al. Twenty-year follow-up of a randomized study comparing breast-conserving surgery with radical mastectomy for early breast cancer. N Engl J Med 2002;347:1227–1232. [PubMed: 12393819]
4. Liljegren G, Holmberg L, Bergh J, et al. 10-year results after sector resection with or without postoperative radiotherapy for stage I breast cancer: a randomized trial. J Clin Oncol 1999;17:2326–2333. [PubMed: 10561294]
5. Polgar C, Fodor J, Major T, et al. Radiotherapy confined to the tumor bed following breast conserving surgery. Strahlenther Onkol 2002;178:597–606. [PubMed: 12426670]
6. Stewart AJ, O'Farrell DA, Cormack RA, et al. Dose volume histogram analysis of normal structures associated with accelerated partial breast irradiation delivered by high dose rate brachytherapy and comparison with whole breast external beam radiotherapy fields. Radiat Oncol 2008;3:39. [PubMed: 19019216]
7. De Boer M, van Deurzen CH, van Dijck JA, et al. Micrometastases or isolated tumor cells and the outcome of breast cancer. N Engl J Med 2009;361:653–663. [PubMed: 19675329]
8. Hoebers FJ, Borger JH, Hart AA, et al. Primary axillary radiotherapy as axillary treatment in breast-conserving therapy for patients with breast carcinoma and clinically negative axillary lymph nodes. Cancer 2000;88:1633–1642. [PubMed: 10738222]
9. Gabizon, AA. Applications of liposomal drug delivery systems to cancer therapy. In: Amiji, MM., editor. Nanotechnology for cancer therapy. Boca Raton: CRC Press; 2007. p. 595-611.
10. Bao A, Phillips WT, Goins B, et al. Potential use of drug carried-liposomes for cancer therapy via direct intratumoral injection. Int J Pharm 2006;316:162–169. [PubMed: 16580161]
11. Harrington KJ, Rowlinson-Busza G, Syrigos KN, et al. Pegylated liposomes have potential as vehicles for intratumoral and subcutaneous drug delivery. Clin Cancer Res 2000;6:2528–2537. [PubMed: 10873109]
12. Oussoren C, Storm G. Liposomes to target the lymphatics by subcutaneous administration. Adv Drug Deliv Rev 2001;50:143–156. [PubMed: 11489337]
13. Velinova M, Read N, Kirby C, et al. Morphological observations on the fate of liposomes in the regional lymph nodes after footpad injection into rats. Biochim Biophys Acta 1996;1299:207–215. [PubMed: 8555266]
14. Bao A, Zhao X, Phillips WT, et al. Theoretical study of the influence of a heterogeneous activity distribution on intratumoral absorbed dose distribution. Med Phys 2005;32:200–208. [PubMed: 15719971]
15. Giap HB, Macey DJ, Bayouth JE, et al. Validation of a dose-point kernel convolution technique for internal dosimetry. Phys Med Biol 1995;40:365–381. [PubMed: 7732068]
16. Kawrakow, I.; Rogers, DW. Technical report PIRS-701. National Research Council of Canada; Ottawa, Canada: 2000. The EGSnrc code system: Monte Carlo simulation of electron and photon transport.
17. Rogers, DW.; Kawrakow, I.; Seuntjens, JP., et al. Technical report PIRS-702. National Research Council of Canada; Ottawa, Canada: 2003. NRC user codes for EGSnrc.
18. Data produced using the MIRD Program, and extracted from the Evaluated Nuclear Structure Data File (ENSDF), 12/15/2008. Additional calculations performed by the program RADLST, Burrows

TW. The program RADLST, Report BNL-NCS-52142. National Nuclear Data Center, Brookhaven National Laboratory; USA: 1988.

19. Stabin MG, da Luz L. Decay data for internal and external dose assessment. Health Phys 2002;83:471–475. [PubMed: 12240721]
20. Mainegra-Hing E, Rogers DW, Kawrakow I. Calculation of photon energy deposition kernels and electron dose point kernels in water. Med Phys 2005;32:685–699. [PubMed: 15839340]
21. Furhang EE, Sgouros G, Chui CS. Radionuclide photon dose kernels for internal emitter dosimetry. Med Phys 1996;23:759–764. [PubMed: 8724750]
22. Simpkin DJ, Mackie TR. EGS4 Monte Carlo determination of the beta dose kernel in water. Med Phys 1990;17:179–186. [PubMed: 2333044]
23. Prestwich WV, Nunes J, Kwok CS. Beta dose point kernels for radionuclides of potential use in radioimmunotherapy. J Nucl Med 1989;30:1036–1046. [PubMed: 2738686]
24. Mackie TR, Bielajew AF, Rogers DW, et al. Generation of photon energy deposition kernels using the EGS Monte Carlo code. Phys Med Biol 1988;33:1–20. [PubMed: 3353444]
25. Harris EJ, Donovan EM, Yarnold JR, et al. Characterization of target volume changes during breast radiotherapy using implanted fiducial markers and portal imaging. Int J Radiat Oncol Biol Phys 2009;73:958–966. [PubMed: 19215828]
26. Rink T, Heuser T, Fitz H, et al. Lymphopscintigraphic sentinel node imaging and gamma probe detection in breast cancer with Tc-99m nanocolloidal albumin: results of an optimized protocol. Clin Nucl Med 2001;26:293–298. [PubMed: 11290886]
27. Wang SX, Bao A, Herrera SJ, et al. Intraoperative 186Re-liposome radionuclide therapy in a head and neck squamous cell carcinoma xenograft positive surgical margin model. Clin Cancer Res 2008;14:3975–3983. [PubMed: 18559620]
28. Samad A, Sultana Y, Aqil M. Liposomal drug delivery: An update review. Curr Drug Deliv 2007;4:297–305. [PubMed: 17979650]
29. Wang SX, Bao A, Phillips WT, et al. Intraoperative therapy with liposomal drug delivery: retention and distribution in human hean and neck squamous cell carcinoma xenograft model. Int J Pharm 2009;373:156–164. [PubMed: 19429301]
30. Campbell, RB. Positively-charged liposomes for targeting tumor vasculature. In: Amiji, MM., editor. Nanotechnology for cancer therapy. Boca Raton: CRC Press; 2007. p. 613-627.
31. Sood A, Yousef IM, Heiba SI, et al. Alternative lymphatic pathway after previous axillary node dissection in recurrent/primary breast cancer. Clin Nucl Med 2004;29:698–702. [PubMed: 15483481]
32. Agarwal A, Heron DE, Sumkin J, et al. Contralateral uptake and metastases in sentinel lymph node mapping for recurrent breast cancer. J Surg Oncol 2005;92:4–8. [PubMed: 16180213]
33. Brashears JH, Dragun AE, Jenrette JM. Late chest wall toxicity after MammoSite breast brachytherapy. Brachytherapy 2009;8:19–25. [PubMed: 18955019]
34. Keisch M, Vicini F, Kuske RR, et al. Initial clinical experience with the MammoSite breast brachytherapy applicator in women with early-stage breast cancer treated with breast-conserving therapy. Int J Radiat Oncol Biol Phys 2003;55:289–293. [PubMed: 12527040]
35. Tobias JS, Vaidya JS, Keshtgar M, et al. Breast-conserving surgery with intra-operative radiotherapy: the right approach for the 21st century? Clin Oncol (R Coll Radiol) 2006;18:220–228. [PubMed: 16605053]
36. Gump FE. Multicentricity in early breast cancer. Semin Surg Oncol 1992;8:117–121. [PubMed: 1496220]
37. Holland R, Veling SH, Mravunac M, et al. Histologic multifocality of Tis, T1-2 breast carcinomas. Implications for clinical trials of breast-conserving surgery. Cancer 1985;56:979–990. [PubMed: 2990668]
38. Belletti B, Vaidya JS, D'Andrea S, et al. Targeted intraoperative radiotherapy impairs the sitmulation of breast cancer cell proliferation and invasion caused by surgical wounding. Clin Cancer Res 2008;14:1325–1332. [PubMed: 18316551]
39. Motomura K, Koyama H, Noguchi S, et al. Malignant seeding of the lumpectomy cavity upon breast-conserving surgery. Oncology 1999;57:121–126. [PubMed: 10461058]

40. Sabel MS, Rogers K, Griffith K, et al. Residual disease after re-excision lumpectomy for close margins. J Surg Oncol 2009;99:99–103. [PubMed: 19065638]

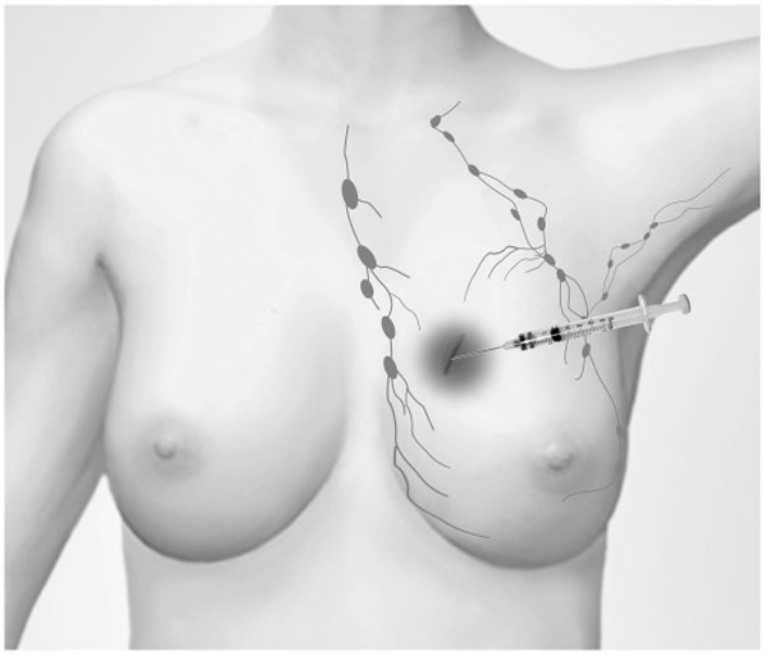

Fig. 1.

Schematic diagram outlining the treatment design. Radionuclides encapsulated within liposomes are injected into lumpectomy cavity in breast. Sustained retention of liposomal radionuclides in the cavity, as well as the gradual clearance and retention in draining lymphatics provide focal brachytherapy to areas where cancer recurrence will most likely occur.

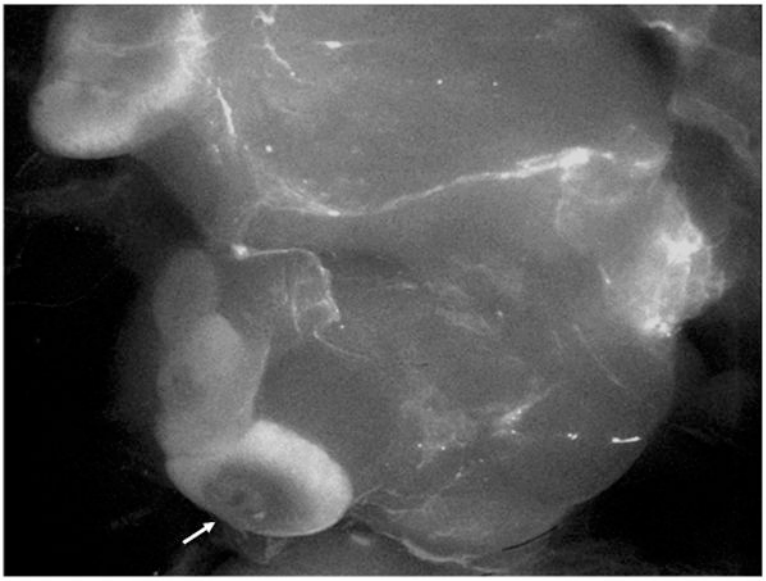

Fig. 2.
Fluorescent image of the distribution of rhodamine B-liposomes in rat lymphatics following intracavitary injection. Arrow points to a draining lymph node.

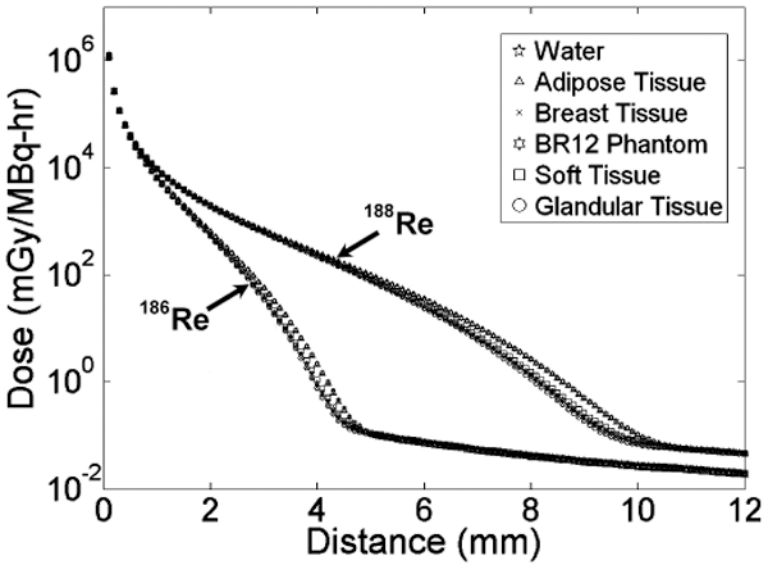

Fig. 3.
Calculated dose point kernels for materials which may represent breast tissue.

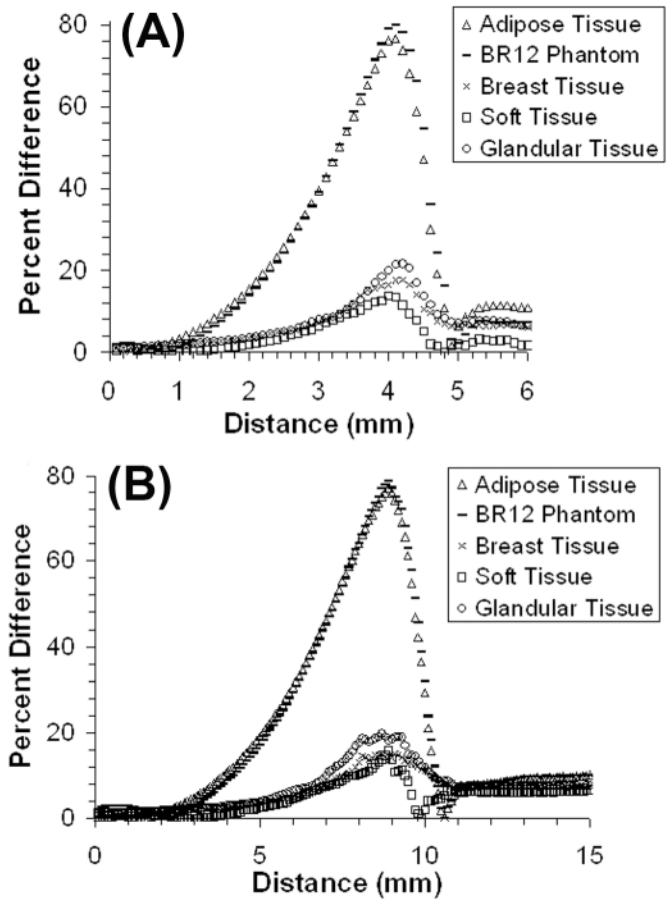

Fig. 4.

Percent differences versus distance with respect to water between dose point kernels for tissues representing breast tissue for ^{186}Re-liposomes (A) and ^{188}Re-liposomes (B).

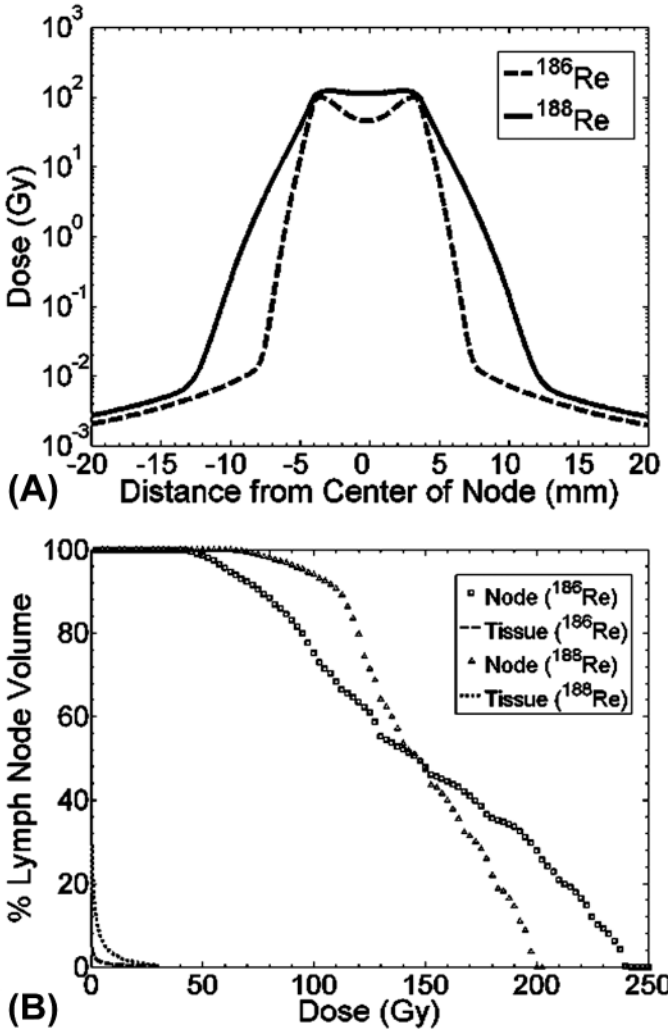

Fig. 5.

Dose profile (A) across center slice of lymph node and dose volume histogram (B) of lymph node and surrounding 1 cm of healthy tissue.

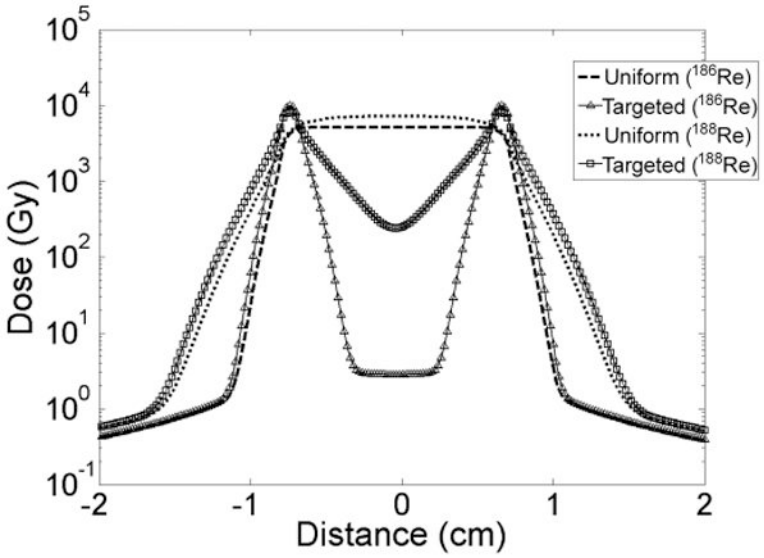

Fig. 6.

Dose profiles across center slice of spherical lumpectomy cavities with uniform or targeted liposome distribution.

Table 1
Dose description for lymph node and surrounding tissue

Tissue	Dose Description	^{186}Re-liposomes	^{188}Re-liposomes
Lymph Node	Avg. Dose (Gy)	150.2	148.3
	Max. Dose (Gy)	240.3	199.7
	Min. Dose (Gy)	39.6	53.8
Surrounding Tissue	Avg. Dose (Gy, 1 mm)	26.4	41.0
	Avg. Dose (Gy, 5 mm)	1.4	6.0
	Avg. Dose (Gy, 10 mm)	0.3	1.3

Table 2
Dose distributions seen in the surrounding tissue of spherical lumpectomy cavities

	^{186}Re-liposomes	
Distance from Cavity (mm)	**1.0 cm Diameter Dose (Gy)**	**1.5 cm Diameter Dose (Gy)**
1	524.8	235.8
2	47.1	23.8
3	3.8	2.4
10	0.6	0.5
Avg. Dose within 2 mm	1503.9	506.7
Injected Activity (mCi)	29.1	29.1
	^{188}Re-liposomes	
Distance from Cavity (mm)	1.0 cm Diameter Dose (Gy)	1.5 cm Diameter Dose (Gy)
1	2559.3	1004.9
4	135.2	58.2
5	41.9	18.9
10	0.9	0.69
Avg. Dose within 5 mm	1122.4	441.6
Injected Activity (mCi)	42.9	42.9

Table 3

Dose distributions seen in the surrounding tissue of irregular shaped ellipsoidal lumpectomy cavities

	^{186}Re-liposomes	
Distance from Cavity (mm)	**Long Axis Dose (Gy)**	**Short Axis Dose (Gy)**
1	105.3	174.5
2	9	17.1
3	1	2.1
10	0.3	0.5
Injected Activity (mCi)	29.1	29.1
	^{188}Re-liposomes	
Distance from Cavity (mm)	Long Axis Dose (Gy)	Short Axis Dose (Gy)
1	451.5	952.9
4	21	58.3
5	6.6	19
10	0.4	0.8
Injected Activity (mCi)	42.9	42.9

Table 4

Dose distribution comparison between uniform cumulative activity distribution and cumulative activity distribution of targeting liposomes for spherical lumpectomy cavity

	^{186}Re-liposomes	
Distance from Cavity (mm)	**Dose of Uniform Distribution (Gy)**	**Dose of Targeted Distribution (Gy)**
1	235.8	611.6
2	23.8	62.6
3	2.4	4.2
10	0.5	0.5
Avg. Dose within 2 mm	506.7	1289
Injected Activity (mCi)	29.1	29.1
	^{188}Re-liposomes	
Distance from Cavity (mm)	Dose of Uniform Distribution (Gy)	Dose of Targeted Distribution (Gy)
1	1004.9	1780.8
4	58.2	117.7
5	18.9	39.8
10	0.69	0.71
Avg. Dose within 5 mm	441.6	805.4
Injected Activity (mCi)	42.9	42.9